New REMPI observations and analyses for Rydberg and ion-pair states of HI

Helgi Rafn Hróðmarsson, Huasheng Wang, Ágúst Kvaran *

Science Institute, University of Iceland, Dunhagi 3, 107 Reykjavík, Iceland

ABSTRACT

Two-dimensional REMPI data, obtained by recording ion mass spectra for HI as a function of two-photon wavenumber were recorded and analyzed. Several previously observed spectra due to resonance transitions to $\Omega = 0$ states were (re)assigned. The spectral data revealed several previously unobserved $(2 + n)$ REMPI spectra. These were assigned and analyzed to derive band origins and rotational parameters of Rydberg and ion-pair states. Perturbation effects, showing as line-shifts and/or signal intensity alterations, were found to be helpful in spectra assignments.

© 2013 Elsevier Inc. All rights reserved.

1. Introduction

Rotational and vibrational structures in electronically excited states of the hydrogen halides are of great spectroscopic interest. Since the original work by Price [1] on the hydrogen halides, an abundance of spectroscopic data and identities have been derived and studied. These studies include standard absorption measurements [2–6], fluorescence studies [6] and resonance enhanced multiphoton ionization (REMPI) experiments [7–22]. A majority of previous studies of the hydrogen halides has placed emphasis on HCl [2,4,6–13,15,16,23–29], whereas the other halide counterparts HBr [5,15–17,22,29–36] and HI [15,16,37–41] have been studied to a lesser extent.

An extensive study of HI and DI was reported by Ginter et al. [38,42] in 1982. Therein, a broad band of excited states was reported and a large number of spectral lines assigned from single photon absorption spectra. Numerous perturbations due to state interactions were observed but none were analyzed quantitatively. Observations were restricted by single-photon selection rules. Later, Wright and McDonald [40] and Pratt and Ginter [41] published REMPI data for resonance two-photon excitations of HI and provided additional spectroscopic information about the molecule. Thus, for example, spectra due to previously unobserved $\Omega = 0^+ - X^1\Sigma^+$ and $I^1\Delta_2 - X^1\Sigma^+$ transitions to excited Rydberg states were observed. However, the $\Omega = 0^+$ state was not characterized any further. Previously identified states of HI as well as states dealt with in this work are characterized in Table 1.

Different notations for the excited states of the hydrogen halides are adopted by Ginter et al. [38] and Callaghan and Gordon [32]. In Table 1 we use the notation adopted by Callaghan et al., where the nature of the excited molecular orbital is specified (σ, π, δ) as well as the halogen atom orbitals involved (s, p, d) along with the ion core configurations. A clear exception to this rule is the V-state which is an ion-pair state.

Whereas most of the studies of HI have focused on spectral assignments and the energetics of the Rydberg and ion-pair states, no emphasis has been placed on spectral perturbations. All the hydrogen halide spectra are rich in intensity deviations and line shifts due to perturbation effects. This makes them ideal for the study of state mixing and photo-fragmentation processes. Furthermore, perturbation effects have been shown to be valuable in spectra assignments [35]. In recent years, a number of papers have been published, which place emphasis on state interactions, energy transfers and photo dissociation processes, in HCl [24,27–29,43–48] and HBr [29,35,36]. Interactions between ion-pair vibrational states and Rydberg states can be organized into three main categories:

(a) Very weak near-resonance state interactions, distinguishable by negligible rotational line shifts but significant alterations in signal line intensities [27,35], observed for triplet Rydberg states and $\Delta\Omega > 0$ state interactions.
(b) Weak near-resonance state interactions, distinguishable by localized line shifts (hence energy level shifts), as well as alterations in signal line intensities [24,26], observed for singlet states and $\Delta\Omega > 0$ state interactions.

---

* Corresponding author. Fax: +354 552 8911 (main office).
  E-mail address: agust@hi.is (Á. Kvaran).

Table 1
Electron configurations and corresponding electronic states for HI.

Configurations Callaghan et al. [32]	Corresponding singlet states	Corresponding triplet states
$(\sigma^2\pi^4)^*$	$X^1\Sigma^+ (0^+)$	None
$(\sigma^2\pi^3)\sigma^*$	$A^1\Pi (1)$	$a^3\Pi (2,1,0^\pm)$
$(\sigma\pi^4)\sigma^*$	$V^1\Sigma^+ (0^+)$	$t^3\Sigma^+ (1,0^-)$
$(\sigma^2\pi^3)6s\sigma$	$C^1\Pi (1)$	$b^3\Pi (2,1,0^\pm)$
$(\sigma^2\pi^3)6p\sigma$	$D^1\Pi (1)$	$d^3\Pi (2,1,0^\pm)$
$(\sigma^2\pi^3)6p\pi$	$E^1\Sigma^+ (0^+)$	$e^3\Sigma^+ (1,0^-)$
	$F^1\Delta (2)$	$f^3\Delta (3,2,1)$
	$G^1\Sigma^- (0^-)$	$g^3\Sigma^- (1,0^+)$
$(\sigma^2\pi^3)5d\pi$	$H^1\Sigma^+ (0^+)$	$h^3\Sigma^+ (1,0^-)$
	$I^1\Delta (2)$	$i^3\Delta (3,2,1)$
	$J^1\Sigma^- (0^-)$	$j^3\Sigma^- (1,0^+)$
$(\sigma^2\pi^3)5d\sigma$	$N^1\Pi (1)$	$n^3\Pi (2,1,0^\pm)$
$(\sigma^2\pi^3)5d\delta$	$K^1\Pi (1)$	$k^3\Pi (2,1,0^\pm)$
	$L^1\Phi (3)$	$l^3 \Phi (4,3,2)$
$(\sigma^2\pi^3)7s\sigma$	$M^1\Pi (1)$	$m^3\Pi (2,1,0^\pm)$
$(\sigma^2\pi^3)7p\sigma$	$R^1\Pi (1)$	$r^3\Pi (2,1,0^\pm)$
$(\sigma^2\pi^3)4f\pi$	$O^1\Sigma^+ (0^+)$	$^3\Sigma^+ (1,0^-)$
	$^1\Delta (2)$	$^3\Delta (3,2,1)$
	$^1\Sigma^- (0^-)$	$^3\Sigma^- (1,0^+)$

(c) Medium to strong off-resonance state interactions, distinguishable by large scale line- and energy level shifts, as well as alterations in signal intensities [26], observed for triplet and singlet states and $\Delta\Omega = 0$ state interactions.

We will now present two-dimensional REMPI data within the two-photon excitation region 69 600–71 500 cm^{-1} for HI and interpretations relevant to new spectroscopic identifications. An energy level diagram of all known states, including new states presented in this paper, is given in Fig. 1.

2. Experimental

Mass resolved REMPI data, referred to as "Two dimensional (2D) REMPI data" (see below) were recorded for a HI molecular beam, created by jet expansion of a pure sample through a pulsed nozzle. Apparatus used is similar to that described elsewhere [24–28,49,50]. Excitation radiation was generated by pulsed excimer laser-pumped dye laser systems, using a Lambda Physik COMPex 205 excimer laser and a Coherent ScanMatePro dye laser. Frequency doubled radiation was focused on the molecular beam inside an ionization chamber between a repeller and extractor plates. Ions formed by multiphoton excitations were directed into a time-of-flight tube and detected by a micro-channel plates (MCP's) detector. Signals were fed into a LeCroy WaveSurfer 44MXs-A, 400 MHz storage oscilloscope and stored as a function of ion time-of-flights and laser radiation wavenumbers. Average signal

Table 2
Typical equipment/condition parameters for REMPI experiments.

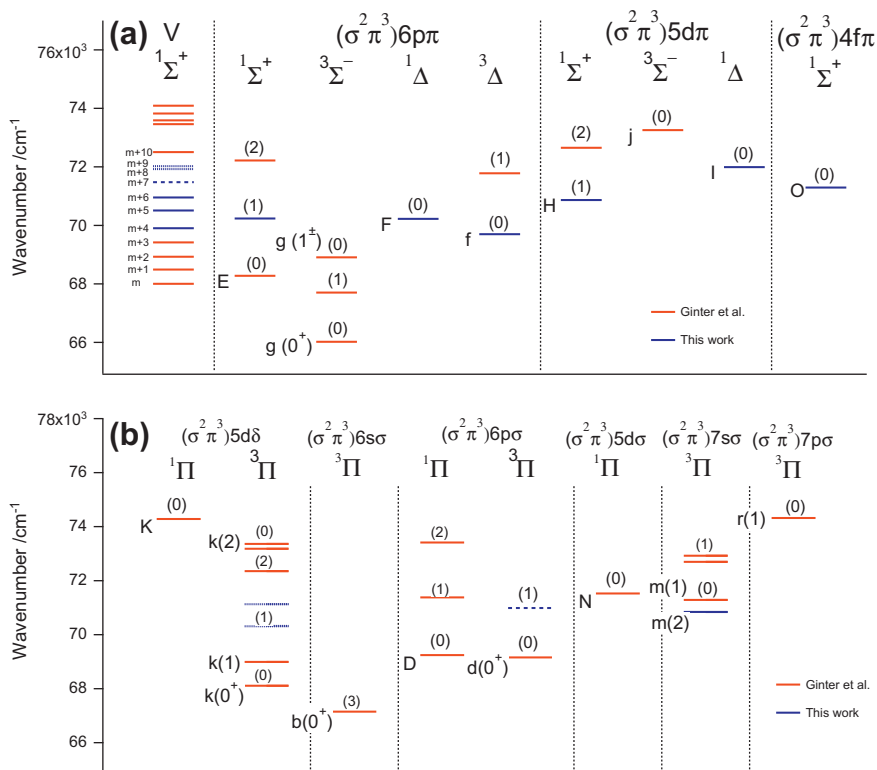|	
HI gas sample	Matheson gas products Inc.
Laser dye	C540A
Frequency doubling crystal	Sirah BBO-2
Laser repetition rate	10 Hz
Dye laser bandwidth	0.095 cm^{-1}
Intensity repetition used	0.1–0.3 mJ/pulse
Nozzle size	500 μm
Sample backing pressure	2.0–2.5 bar
Pressure inside ionization chamber	10^{-6} mbar
Nozzle opening time	150–200 μs
Delay time for laser excitation	450–550 μs
Excitation wavenumber step sizes	0.05–0.10 cm^{-1}
Time of flight step sizes	10 ns

Fig. 1. Energy level diagram of all the known electronic states for HI. The ion-pair states and the $^{1,3}\Sigma$ and $^{1,3}\Delta$ Rydberg states with π Rydberg electrons are presented in (a). The $^{1,3}\Pi$ Rydberg states with σ and δ Rydberg electrons are in (b). Red lines correspond to previously detected bands [38] whereas blue lines correspond to states observed in this work, some of which have been detected before (see text). Dotted lines correspond to states that have been previously detected in single-photon spectroscopy but not in REMPI whereas dashed lines correspond to bands that have neither been detected in single-photon spectroscopy or in REMPI. Vibrational numberings are shown in parenthesis on top of every line for the Rydberg states. Vibrational levels for the V states are labeled as $v' = m + i$; $i = 0,1,2,....$ (For interpretation of the references to color in this figure legend, the reader is referred to the web version of this article.)

levels were evaluated and recorded for a fixed number of laser pulses. The data were corrected for laser power and mass calibrated to obtain ion yields as a function of mass and excitation wavenumber (2D-REMPI data). REMPI spectra for certain ions as a function of excitation wavenumber (1D-REMPI) were obtained by integrating mass signal intensities for the particular ions. Care was taken to prevent saturation effects as well as power broadening by minimizing laser power. Laser calibration was based on an optogalvanic spectrum, obtained from a built-in neon cell as well as on observed (2 + 1) iodine atom REMPI peaks [51]. The accuracy of the calibration was typically found to be about ±0.5 cm^{-1} on a laser wavenumber scale, hence about ±2.0 cm^{-1} on a two-photon wavenumber scale. Equipment parameters are listed in Table 2.

3. Results and analysis

Most HI spectra, previously detected in the excitation region 69 600–71 500 cm^{-1}, were identified and assigned. Spectra which have been assigned [38] to resonance transitions to the $E^1\Sigma^+$ and $H^1\Sigma^+$ Rydberg states were reassigned (see below). Partly unassigned spectrum at $v^0 = 71\,295$ cm^{-1} was fully assigned (see below). In addition, several "new spectra" and/or "new lines" were observed and assigned. These can be categorized into four main groups (see Table 3 and Fig. 2):

(i) Spectra due to two-photon resonance transitions to Rydberg states not previously detected in REMPI [41] but identified in single-photon absorption studies [38].

(ii) Spectra due to two-photon resonance transitions to Rydberg states, not previously detected.

(iii) Spectra due to two-photon resonance transitions to ion-pair states, not previously detected in REMPI [41] but identified in single-photon absorption studies [38].

(iv) Spectra due to two-photon resonance transitions to ion-pair states not previously detected.

Spectroscopic parameters of all observed states are summarized in Table 3. Newly observed states are marked specifically according

to the categories mentioned above (i–iv). Corresponding rotational lines are listed in Table 4. In Fig. 2, the relevant 1D-REMPI spectra for parent and fragment ions are shown. The $k^3\Pi_0(v' = 1)$ Rydberg state spectrum, which previously has been identified in single-photon absorption spectroscopy [38], but not in two-photon REMPI, is shown in Fig. 2a along with some of the R and S lines of the nearby $F^1\Delta_2(v' = 0)$ spectra. Another Rydberg state spectrum, also identified previously in single-photon absorption, for the $k^3\Pi_1(v' = 1)$ state, is shown in Fig. 2b as well as the previously undetected $d^3\Pi_0(v' = 1)$ band, which Q lines in the I$^+$ spectrum coincide partly with a strong atomic iodine line at 70988.2 cm^{-1}. In Fig. 2c the previously unreported $V^1\Sigma^+(v' = m + 7)$ ion-pair state spectrum is shown along with the S lines of the $O^1\Sigma^+(v' = 0)$ state spectrum [41]. The ion-pair states spectra for $V^1\Sigma^+(v' = m + 8)$ and $V^1\Sigma^+(v' = m + 9)$ were detected in the spectral region shown in Fig. 2d, where the $I^1\Delta_2(v' = 0)$ spectrum also appears [41]. For clarity reason, the H$^+$ fragment spectrum from Fig. 2d is enlarged in Fig. 2e.

3.1. Spectra due to resonance transitions to the $H^1\Sigma^+$ and $E^1\Sigma^+$ Rydberg states; reassignments

Ginter et al. [38] assign the $v^0 = 70850.5$ cm^{-1} and 72650.8 cm^{-1} bands to the $E^1\Sigma^+((\sigma^2\pi^3)6p\pi)$, $v' = 0$ and 1 Rydberg states respectively and the $v^0 = 68277.3$ cm^{-1}, 70242.1 cm^{-1} and 72217.6 cm^{-1} bands to the $H^1\Sigma^+((\sigma^2\pi^3)5d\pi$, $v' = 0$, 1, and 2 Rydberg states respectively without any clear arguments. This we believe that should be reassigned such that the $v^0 = 68277.3$ cm^{-1}, 70242.1 cm^{-1} and 72217.6 cm^{-1} bands correspond to the $E^1\Sigma^+((\sigma^2\pi^3)6p\pi)$, $v' = 0$, 1, and 2 Rydberg states, respectively and that the $v^0 = 70850.5$ cm^{-1} and 72650.8 cm^{-1} bands belong to the $H^1\Sigma^+((\sigma^2\pi^3)5d\pi)$, $v' = 1$ and 2 states, respectively, for the following reasons (a–c):

(a) Based on comparison with HCl [8–11] and HBr [32] the energies of the E states are lower than those of the corresponding H states. Thus the band origin differences (Δv^0) between the $v' = 0$ states $(v^0(H(v = 0) - v^0(E(v = 0))$ are found to be 4905 cm^{-1} and 1706 cm^{-1} for HCl and HBr respectively. We therefore believe that the lower energy $\Omega = 0^+$ serie

Table 3
HI: Band origin (v^0) and rotational parameters (B_v and D_v) for all states observed in the 69 600–72 100 cm^{-1} excitation region. The identifications (i)–(iv) are according to a categorization specified in the text.

States[c]	v^0 (cm^{-1})		B_v (cm^{-1})		$D_v \times 10^4$ (cm^{-1})		Identification
	This work[e]	Others	This work	Others	This work	Others	
$f^3\Delta_1$ (0)	69699.9	69687.0[a]	6.31 ± 0.02	6.135	4.6 ± 1.0	1.92	
$V^1\Sigma^+$ ($m + 4$)	69903.3	69909.9[a]	2.94 ± 0.18	3.27	10 ± 40	6,5	
$F^1\Delta_2$ (0)	70223.6	70228.3[a]	6.32 ± 0.01	6.30	2.6 ± 0.6	1.2	
$E^1\Sigma^+$ (1)[d]	70236.1	70242.1[a]	6.34 ± 0.01	5.95	1100 ± 20	125	
$k^3\Pi_0$ (1)	70310.8	70320.4[a]	5.13 ± 0.03	5.058	−4 ± 9	−21.0	(i)
$V^1\Sigma^+$ ($m + 5$)	70511.0	70512[a]	3.66 ± 0.02	3.800	83 ± 4	−70.2	(i)
$m^3\Pi_2$ (0)	70841.5	70837.6[a]	6.21 ± 0.04	6.11	12 ± 5	1.94	
$H^1\Sigma^+$ (0)[d]	70866.3	70850.5[a]	5.94 ± 0.17	6.00	−11 ± 21	128	
$V^1\Sigma^+$ ($m + 6$)	70952.3	70948.6[a]	3.56 ± 0.10	4.09	24 ± 10	44	
$d^3\Pi_0$ (1)	70988.2	–	5.79 ± 0.12	–	−290 ± 40	–	(ii)
$k^3\Pi_1$ (1)	71126.4	71125.0[a]	6.22 ± 0.02	6.30	−2.6 ± 1.6	4.82	(i)
$m^3\Pi_1$ (0)	–	71287.3[a]	–	6.254	–	3.18	
$O^1\Sigma^+$ (0)[d]	71294.7	71301.9[b]	6.25 ± 0.22	5.82	33 ± 26	–	
$D^1\Pi$ (1)	–	71382.4[a]	–	6.052	–	1.92	
$V^1\Sigma^+$ ($m + 7$)	71478.4	–	2.95 ± 0.10	–	−4 ± 5	–	(iv)
$N^1\Pi$ (0)	–	71526.2[a]	–	6.163	–	1.74	
$f^3\Delta$ (1)	–	71780.5[a]	–	5.957	–	9.73	
$V^1\Sigma^+$ ($m + 8$)	71924.4	71920.3[a]	4.17 ± 0.17	3.97	270 ± 70	158	(iii)
$I^1\Delta_2$ (0)	71989.4	71990[b]	6.31 ± 0.01	6.312	2.4 ± 0.1	2.7	
$V^1\Sigma^+$ ($m + 9$)	72023.2	72022.4[a]	2.84 ± 0.03	2.792	1 ± 4	−4.61	(iii)

[a] Ref. [38].
[b] Ref. [41].
[c] Term symbol (vibrational quantum numbers).
[d] (Re)assigned.
[e] v^0 for $\Omega = 0$ states equal observed v for the $J' = 0 \longleftarrow\longleftarrow J'' = 0$ transitions; v^0 for $\Omega > 0$ were derived from fitting of observed rotational lines ($J' > 0$).
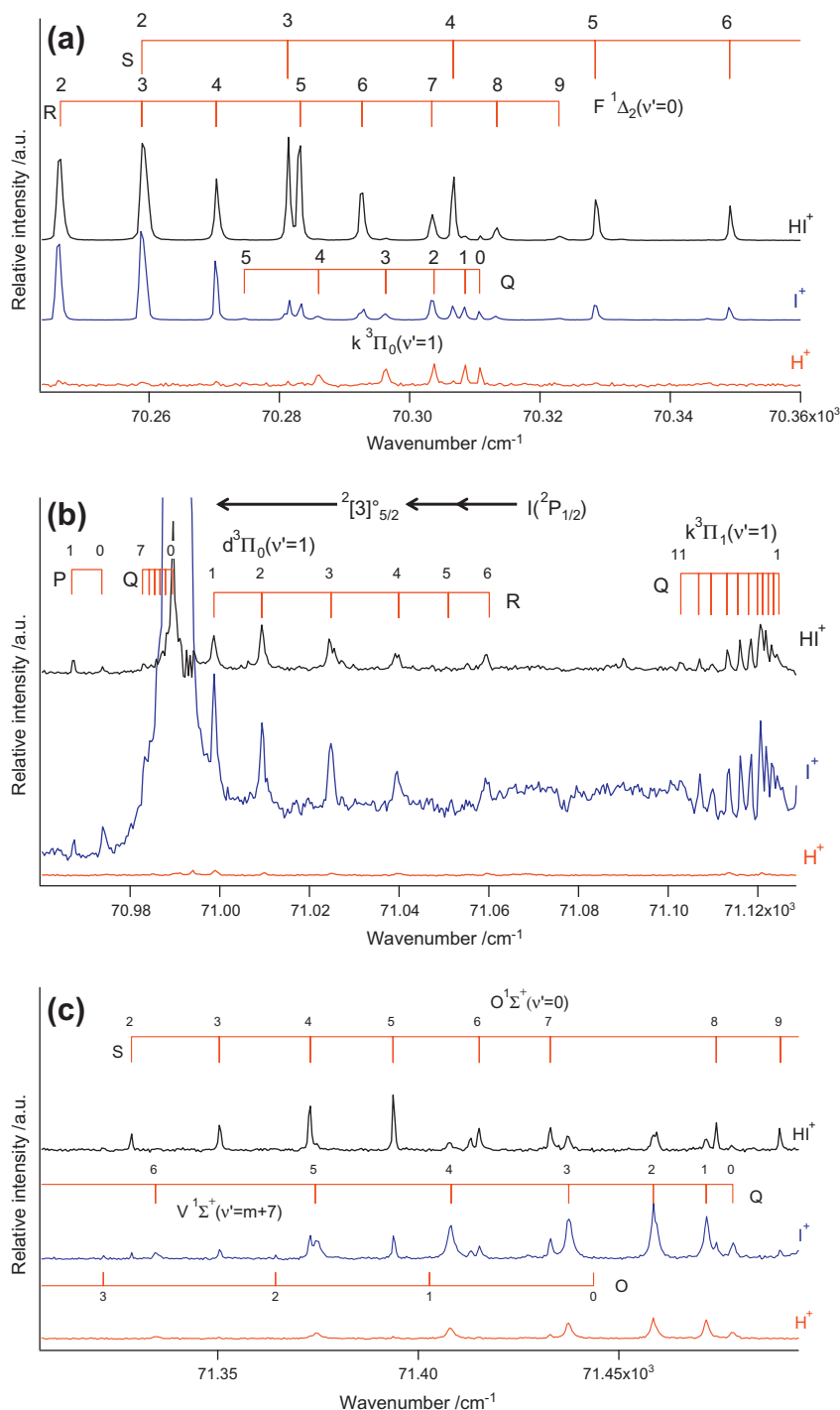
Fig. 2. 1D-REMPI spectra for H$^+$, I$^+$, and HI$^+$ and J' assignments of rotational peaks corresponding to two-photon resonance excitations to $F^1\Delta_2(v' = 0)$ (a), $k^3\Pi_0(v' = 1)$ (a), $d^3\Pi_0(v' = 1)$ (b), $k^3\Pi_1(v' = 1)$ (b), $O^1\Sigma^+(v' = 0)$ (c), $V^1\Sigma^+(v' = m + 7)$ (c), $V^1\Sigma^+(v' = m + 8)$ (d and e), $I^1\Delta_2(v' = 0)$ (d), and $V^1\Sigma^+(v' = m + 9)$ (d and e). In Fig. 2e, the H$^+$ spectrum from Fig. 2d is intensified to show the presence of the ion-pair states $V^1\Sigma^+(v' = m + 7)$ and $V^1\Sigma^+(v' = m + 8)$ more clearly.

(v^0 = 68277.3 cm^{-1}, 70242.1 cm^{-1} and 72217.6 cm^{-1} bands) belongs to $E^1\Sigma^+((\sigma^2\pi^3)6p\pi)$ whereas the higher energy serie (v^0 = 70850.5 cm^{-1} and 72650.8 cm^{-1}) is for $H^1\Sigma^+((\sigma^2\pi^3)5$-$d\pi)$. If, on the other hand, the v^0 = 68277.3 cm^{-1} band belongs to $E(v = 0)$ and that the v^0 = 70850.5 cm^{-1} is for $H(v = 0)$, Δv^0 = 2573.2 cm^{-1}, which contradicts a decreasing Δv^0 as the halogen atom increases (see above). We therefore assign the v^0 = 70850.5 cm^{-1} band to $H(v = 1)$ in which case v^0 for $H(v = 0)$ should be close to 69 000 cm^{-1} and Δv^0 about 720 cm^{-1}. No spectrum for an $\Omega = 0^+$ state in that region has been found yet. Judging from the information concerning the

spectral intensities for the v^0 = 70850.5 cm^{-1} band [38,41], which are marked vvw (very very weak) there is a reason to believe that the spectrum for $H(v = 0)$ is still weaker.

(b) For HCl and HBr it has been found that the interaction strength between E and V states is stronger than any other Rydberg to ion-pair interactions, including the H and V interactions, showing in the form of large line, hence energy level shifts as well as intensity irregularities [24,27–29,35,36]. Thus, characteristic large irregularities in energy gaps between ion-pair vibrational states are found closest in energy to E states for HCl and HBr [15]. This shows as enhancements in
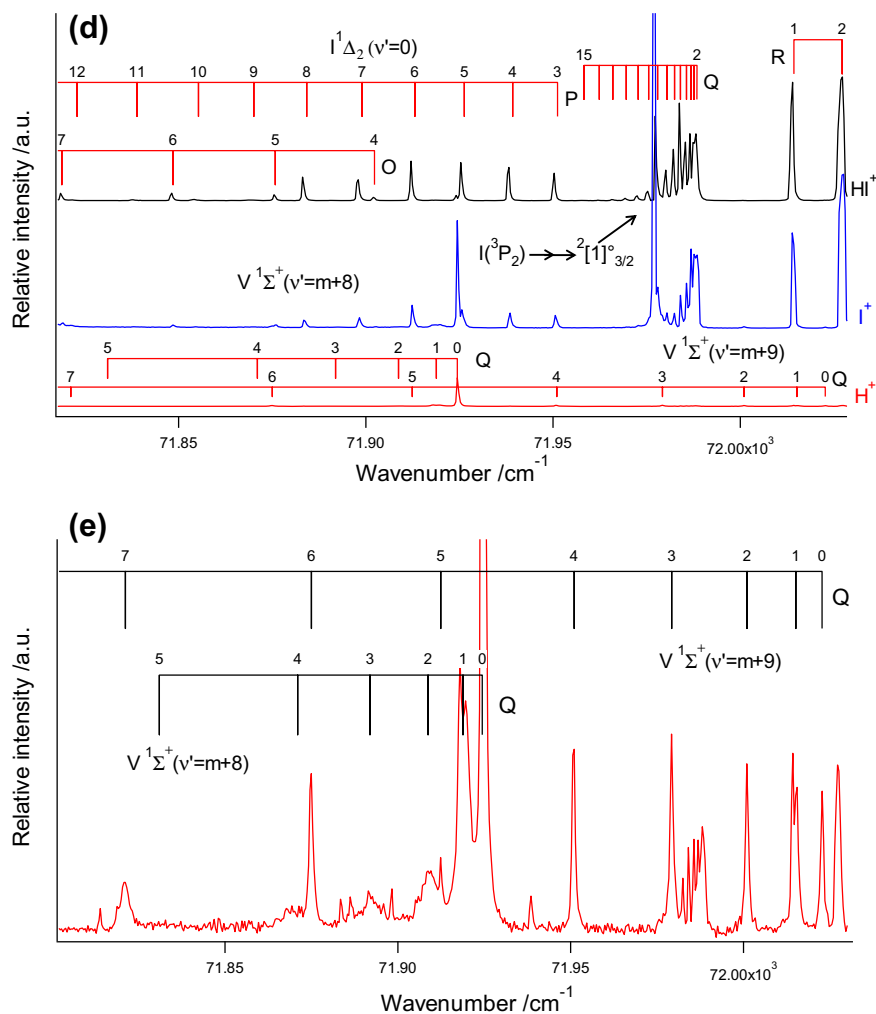
Fig. 2 (continued)

energy gaps between ion-pair vibrational states closest in energy to E states and corresponding lowering in the energy gaps above and below in energy (see Figs. 3 and 5 in Ref. [15]). As shown in Fig. 3 the same effect is seen for HI for the reassigned E state. Thus the energy gaps between $V(v' = m)$ and $V(v' = m + 1)$, $V(v' = m + 4)$ and $V(v' = m + 5)$ as well as between $V(v' = m + 9)$ and $V(v' = m + 10)$ which are closest to the $E(v' = 0)$, $E(v' = 1)$, and $E(v' = 3)$ states, respectively, all are enhanced whereas the energy gaps between $V(v' = m + 1)$ and $V(v' = m + 2)$, $V(v' = m + 3)$ and $V(v' = m + 4)$, $V(v' = m + 5)$ and $V(v' = m + 6)$ as well as $V(v' = m + 8)$ and $V(v' = m + 9)$ all are reduced.

(c) Ion intensity ratios, $I(X^+)/I(HX^+)$ (X = Cl, Br), for Rydberg states, are found to be clear indications of interaction strengths between Rydberg and ion-pair states. Largest values have been found for the E state spectra [29,36]. This also holds for the reassigned E state spectra in the case of HI. Thus, these ratios are typically found to be about 4 for the E state spectra but only about 1 for the reassigned H state spectra.

(d) Quantum defect analysis [35] and comparison with iodine atomic Rydberg states [51] with np^1 and nd^1 configurations further support this assignment.

3.2. The 71 295 cm^{-1} spectrum; assignment

The spectrum observed near 71 295 cm^{-1} has been assigned to an $\Omega = 0^+$ state without any further specifications [41]. The spectrum shows dominating HI$^+$ signals but also significant fragment ion signals (I$^+$ and H$^+$) for large range of J' levels (see S lines in Fig. 2b). This is characteristic for an $\Omega = 0(^1\Sigma^+)$ Rydberg state showing strong homogeneous, off resonance, coupling with ion-pair vibrational state [28,35,36]. Spectral analysis give a rotational constant $B' = 6.25 \pm 0.22$ cm^{-1} and band origin $v^0 = 73294.7$ cm^{-1} (see Table 3). This state can neither be a vibrationally excited E or H state, since it does not fit into the corresponding vibrational state series. Quantum defect analysis [36] show that this state cannot be a $^1\Sigma^+$ state in the E and H Rydberg state series corresponding to excitations to orbitals with higher principal quantum numbers (i.e. not $(s^2p^3)7pp$ and $(\sigma \, ^2\pi \, ^3)6d\pi$ states. Such analysis and comparison with quantum defect values (δ) for iodine atomic Rydberg states [51], on the other hand, suggest that this state could correspond to an excitation to the $4f$ orbital, $v' = 0$ ($\delta \approx 1.0$). We therefore assign the $v^0 = 73295$ cm^{-1} state to $O^1\Sigma^+(v' = 0)$ with the electron configuration $(\sigma^2\pi^3)4f\pi$.

3.3. Spectra due to two-photon resonance transitions to Rydberg states not previously detected in REMPI but identified in single-photon absorption studies

The $k^3\Pi$ Rydberg states correspond to an electron excitation to a $6d\delta$ Rydberg orbital (Table 1). Several vibrational bands for these states have been identified (see Fig. 1b) and analyzed (Table 3 and Ref. [38]). However, in the two-photon REMPI experiments, performed by Pratt and Ginter [41], only $k^3\Pi$ Rydberg bands for

Table 4
Rotational lines for HI due to two-photon resonance transitions to the $k^3\Pi_0(v'=1)$, $k^3\Pi_1(v'=1)$, $d^3\Pi_0(v'=1)$, $V^1\Sigma^+(v'=m+7)$, $V^1\Sigma^+(v'=m+8)$, and $V^1\Sigma^+(v'=m+9)$ states.

J'	$k^3\Pi_0$	$k^3\Pi_1$	$d^3\Pi_0$		
	Q	Q	P	Q	R
0	70310.8			70989.5	70998.5
1	70308.6	71125.4	70973.7	70989.3	71009.2
2	70304.0	71124.1	70967.4	70988.0	71024.6
3	70296.4	71123.1		70986.8	71039.4
4	70286.1	71121.6		70985.7	71051.5
5	70274.7	71120.4		70984.6	71059.0
6		71118.4		70983.0	
7		71115.9		70981.5	
8		71113.2			
9		71109.7			
10		71106.9			
11		71107.2			
	$V^1\Sigma^+(m+7)$		$V^1\Sigma^+(m+8)$	$V^1\Sigma^+(m+9)$	
	O	Q	Q	Q	
0		71478.4	71924.4	72022.7	
1		71471.8	71918.8	72015.5	
2	71443.7	71458.6	71908.7	72001.0	
3	71402.8	71437.5	71890.2	71979.2	
4	71364.4	71408.2	71871.4	71950.6	
5	71321.5	71374.3	71831[a]	71912.4	
6	71265.9	71334.3		71875.0	
7	71214.3	71291[a]		71820.8	
8		71240.6		71769.9	
9		71186.8		71706.8	
10				71631.7	

[a] Uncertainty of peak positions is ±5 cm^{-1}.

the $k^3\Pi_0(v'=2)$ and $k^3\Pi_1(v'=2)$ states were observed. Now the $k^3\Pi_0(v'=1)$ and $k^3\Pi_1(v'=1)$ vibrational bands have been observed in REMPI for the first time (see Fig. 2a and b), centered at $v^0 = 70310.8$ cm^{-1} and 71126.4 cm^{-1} respectively. Spectral analyses give values of rotational constants, B_v and D_v, in good agreement with previously determined values (see Table 3).

No perturbations are observed for the $k^3\Pi_0(v'=1)$ state in terms of line shifts or intensity alterations, in good agreement with the findings of Ginter et al. [38]. For the $k^3\Pi_1(v'=1)$ Rydberg state, on the other hand, Ginter et al. reported that it "may be perturbed at high J'". We observe line shifts for high J' values as well as $I(I^+)/I(HI^+)$ intensity ratios for $J' = 8–11$ (Fig. 4) which is characteristic of near-resonance interactions with an ion-pair state [25–28,35,36] (see Section 3.6).

3.4. Spectra due to two-photon resonance transitions to Rydberg states, not previously detected

A new, previously unobserved spectrum is seen in the two-photon excitation region 70970–71070 cm^{-1} (see Fig. 2b). Clear peaks are observed on the high wavenumber side of a strong iodine atomic line (79991.6 cm^{-1}; $^3[3]^\circ_{5/2} \leftarrow\leftarrow\ ^2P_{1/2}$ transition) in the I^+ spectrum and in the HI^+ spectrum. These peaks are assigned to R lines, whereas the structure in the HI^+ spectrum in the region of the atomic line is assigned to overlapping Q lines. On the short wavenumber side, two P lines are observed. The I^+ signals are found to be stronger than the parent ion signals whereas the H^+ signals are very weak. Furthermore, no significant line shifts or significant changes in the intensity ratios or bandwidths of the spectral lines, as a function J', are observed. This is characteristic of a predissociating Π state. Analysis of the rotational structure revealed an $\Omega = 0$ state, which excludes $^1\Delta$ or $^3\Delta$ states. Furthermore, appearance of R and P lines, rules out a Σ state. We therefore believe that the "new spectrum" corresponds to transitions to a $^3\Pi_0$
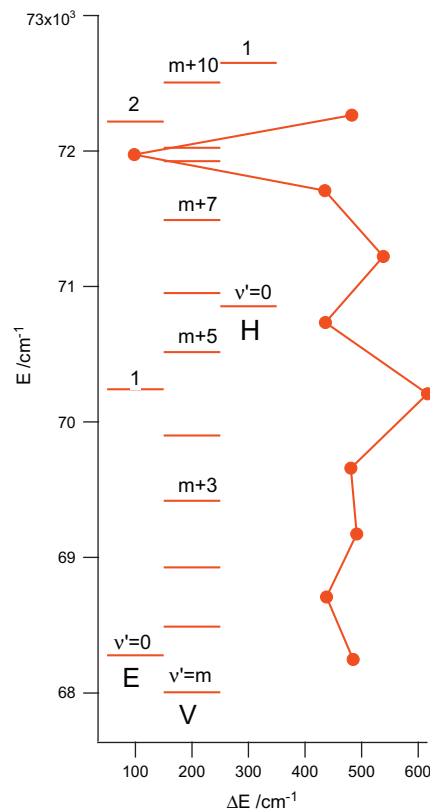

Fig. 3. Vibrational energy levels for the E, H, and $V(^1\Sigma^+)$ states and vibrational level spacings between the V states vs. energy.

state, which could either belong to the $b^3\Pi_0$ or the $d^3\Pi_0$ Rydberg series (see Fig. 1b). The third vibrational band for $b^3\Pi_0$ state has been observed at energies approximately 4000 cm^{-1} lower than the "new state" [38], whereas the first vibrational band ($v'=0$) of $d^3\Pi_0$ has been observed at 69157.8 cm^{-1}. If the "new band" belongs to the second vibrational level ($v'=1$) of the $d^3\Pi_0$ Rydberg state, the energy spacing between the vibrational levels is 1830.4 cm^{-1}, which one might expect for a Rydberg state of HI (see Fig. 1). We therefore assign the "new band" at $v^0 = 70988.2$ cm^{-1} to the $d^3\Pi_0(v'=1)$, $(\sigma^2\pi^3)6p\sigma$ Rydberg state.

3.5. Spectra due to two-photon resonance transitions to ion-pair states, not previously detected in REMPI but identified in single-photon absorption studies

The ion-pair states $V^1\Sigma^+(v'=m+8)$ and $V^1\Sigma^+(v'=m+9)$ have not been detected in two-photon REMPI before. In the REMPI spectra shown in Fig. 2d and e, weak structures are observed which are assigned to the ion-pair states $V^1\Sigma^+(v'=m+8)$ and $V^1\Sigma^+(v'=m+9)$. Strongest signals are found for H^+. Spectral analyses reveal rotational constants, B_v and D_v, as well as spectral origin, v^0, in good agreement with previously determined values [38] (Table 3).

In the work by Ginter et al. [38] the $V^1\Sigma^+(v'=m+8)$ spectrum was found to be perturbed and very diffuse for low J's whereas the $V^1\Sigma^+(v'=m+9)$ spectrum showed sharp lines. This agrees with our findings (see Fig. 2e). The $J'=0$, Q-line for $V^1\Sigma^+(v'=m+8)$ is a sharp peak at 71924.4 cm^{-1}, whereas all other subsequent peaks exhibit clear line broadenings (see Fig. 5). By analogy with HBr and HCl this is most probably associated with interactions with predissociating Rydbergs states [29,35,36]. Several state interactions, involving the V states can be of importance in this energy region (see Fig 6). Thus the $V^1\Sigma^+(v'=m+9)$ will experience
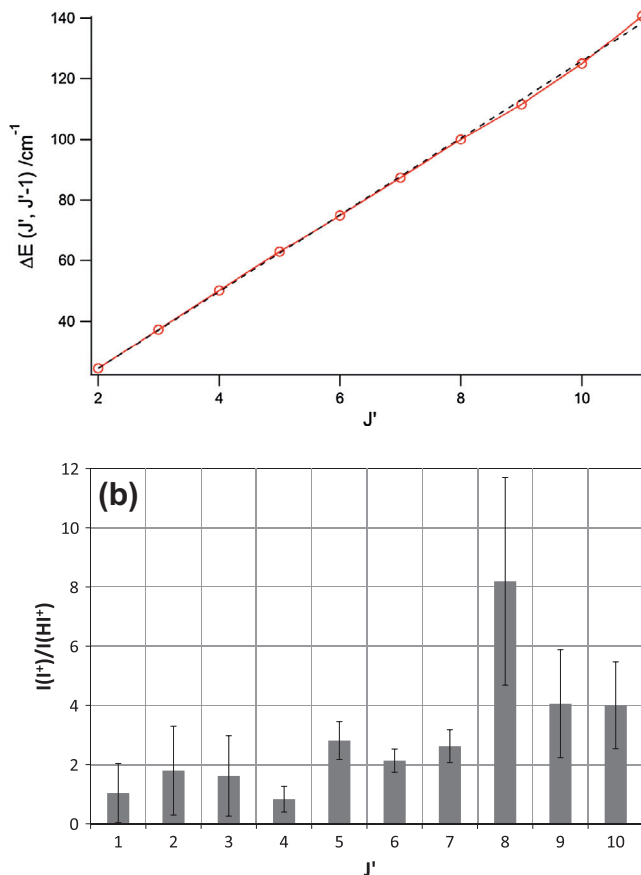
Fig. 4. (a) Energy differences of rotational levels for the $k^3\Pi_1(v' = 1)$ Rydberg state as a function of J'. Perturbations are seen for high J'. (b) Relative ion signal intensities, $I(\text{I}^+)/I(\text{HI}^+)$ vs. J' derived from Q rotational lines of REMPI spectra due to two-photon resonance transitions to the Rydberg state $k^3\Pi_1(v' = 1)$.
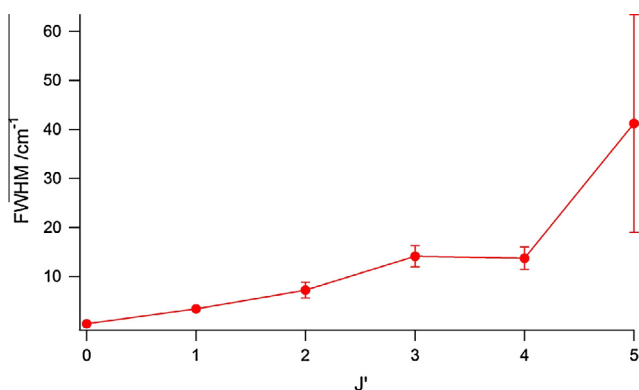

Fig. 5. Rotational line-widths vs. J' derived from the Q lines of the H^+ REMPI spectrum for $V^1\Sigma^+$ ($v' = m + 8$). The large increase in line-widths as J' increases is evidence of a strong off-resonance interaction with another $^1\Sigma^+$state.

off-resonance interactions mainly with the $E^1\Sigma^+(v' = 2)$ state resulting in energy level lowering of the $V^1\Sigma^+(v' = m + 9)$ state whereas the $V^1\Sigma^+(v' = m + 7)$ state (see text below) will mainly experience off-resonance interactions with the $O^1\Sigma^+(v' = 0)$ state resulting in an increase in the energy levels of the $V^1\Sigma^+(v' = m + 7)$ state. The $V^1\Sigma^+(v' = m + 8)$, on the other hand, state may experience significant off-resonance interaction both with the $O^1\Sigma^+(v' = 0)$ and the $E^1\Sigma^+(v' = 2)$ states. As a result, the $V^1\Sigma^+(v' = m + 8)$ state will be "clenched" between the two ion-pair states, $V^1\Sigma^+(v' = m + 7)$ and $V^1\Sigma^+(v' = m + 9)$. This explains the small vibrational energy spacing
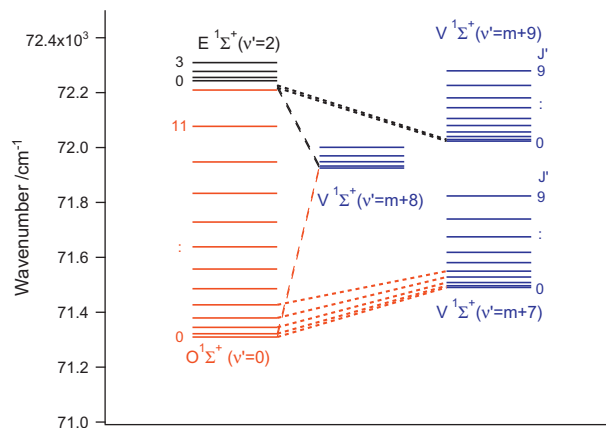

Fig. 6. Rotational energy levels, derived from observed REMPI rotational peaks for the $O^1\Sigma^+$ ($v' = 0$), $V^1\Sigma^+$ ($v' = m + 7$), $V^1\Sigma^+$ ($v' = m + 8$), $V^1\Sigma^+$ ($v' = m + 9$) and $E^1\Sigma^+$ ($v' = 2$) states. The rotational energy levels for the $E^1\Sigma^+$ ($v' = 2$) state were derived from rotational constants reported by Ginter et al. [38]. Proposed off-resonance interaction between the $O^1\Sigma^+$ ($v' = 0$) and the ion-pair states $V^1\Sigma^+$ ($v' = m + 7$) and $V^1\Sigma^+$ ($v' = m + 8$) is indicated by red broken lines by varying thickness as an indication of an alternating state mixing. Likewise, off-resonance interactions between the $E^1\Sigma^+$ ($v' = 2$) and the ion-pair states $V^1\Sigma^+$ ($v' = m + 8$) and $V^1\Sigma^+$ ($v' = m + 9$) is indicated by black broken lines by varying thickness. (For interpretation of the references to color in this figure legend, the reader is referred to the web version of this article.)

between these states (Table 3). Furthermore, the ion-pair state $V^{1-}\Sigma^+(v' = m + 9)$, is found to experience some near-resonance interaction [52].

3.6. Spectra due to two-photon resonance transitions to ion-pair states not previously detected

The ion-pair state $V^1\Sigma^+(v' = m + 7)$ for HI has not been detected or analyzed before. A structure characteristic for an ion-pair state spectrum is observed (Fig 2c) close to the $O^1\Sigma^+$ ($v' = 0$) state spectrum (between the $V^1\Sigma^+(v' = m + 6)$ and $V^1\Sigma^+(v' = m + 8)$ states). It shows medium to strong H^+ and I^+ signals and weak to very weak HI^+ signals as to be expected for an ion-pair state spectrum [25,27–29,35,36]. Spectral analysis give a small rotational constant ($B_v = 2.95 \text{ cm}^{-1}$; see Table 3) of the same order of magnitude as for other ion-pair states. We therefore, assign this newly observed structure to the $V^1\Sigma^+$ ($v' = m + 7$) ion-pair state. As mentioned before, the $V^1\Sigma^+$ ($v' = m + 7$) state will experience off-resonance interactions with the $O^1\Sigma^+$ ($v' = 0$) Rydberg state, which will result in upwards energy level shifts for $V(v' = m + 7)$. Furthermore, the $V(v' = m + 7)$ state must be the perturbing state for the near-resonance interaction effects observed for the $k^3\Pi_1(v' = 1)$ state. $J' = 8$ – 11, mentioned before (see Section 3.3 and Fig. 4).

4. Conclusions

Several spectra features, observed in $(2 + n)$ REMPI of HI, for the excitation region 69 600–71 500 cm^{-1}, were assigned and analyzed. Perturbation effects, seen as line-shifts and/or intensity anomalies, due to interactions between Rydberg states and ion-pair states or repulsive states, proved to be helpful in assigning spectra. Rotational parameters and band origins were determined. Previously observed spectra due to resonance transitions to the $E^1\Sigma^+$ and $H^1\Sigma^+$ Rydberg states were reassigned and the band spectrum centered at $v^0 = 71295 \text{ cm}^{-1}$ was assigned to the $O^1\Sigma^+$ ($v' = 0$), $(\sigma^2\pi^3)4f\pi$ state. Several new spectra were identified and assigned. (i) Firstly, spectra due to resonance transitions to the Rydberg states $k^3\Pi_0(v' = 1)$ and $k^3\Pi_1(v' = 1)$, not previously observed in REMPI,

were identified. Near-resonance interactions are identified for the $k^3\Pi_0(v'=1)$ state. (ii) Secondly, a new spectrum at $v^0 = 70988.2$ cm^{-1}, not previously observed, showing characteristics of predissociating Π Rydberg states is assigned to the $d^3\Pi_0(v'=1)$, $(\sigma^2\pi^3)6p\sigma$ state. (iii) Thirdly, two vibrational bands of the ion-pair state $V^1\Sigma^+$, $V(v'=m+8)$ and $V(v'=m+9)$, which have not been detected in REMPI before, were identified and (iv) finally, a new spectrum due to resonance transition to the $V(v'=m+7)$ vibrational state was observed. All the V state spectra in (iii) and (iv) ($v'=m+7, m+8, m+9$) show characteristic effects of strong off-resonance interactions with the $E^1\Sigma^+$ ($v'=2$) and the $O^1\Sigma^+$ ($v'=0$) states.

Acknowledgments

References

[1] W.C. Price, Proc. Roy. Soc. Ser. A 167 (1938) 216.
[2] S.G. Tilford, M.L. Ginter, J.T. Vanderslice, J. Mol. Spectrosc. 33 (1970) 505–519.
[3] S.G. Tilford, M.L. Ginter, J. Mol. Spectrosc. 40 (1971) 568–579.
[4] D.S. Ginter, M.L. Ginter, J. Mol. Spectrosc. 90 (1981) 177–196.
[5] D.S. Ginter, M.L. Ginter, S.G. Tilford, J. Mol. Spectrosc. 90 (1981) 152.
[6] J.B. Nee, M. Suto, L.C. Lee, J. Chem. Phys. 85 (1986) 719–724.
[7] T.A. Spiglanin, D.W. Chandler, D.H. Parker, Chem. Phys. Lett. 137 (1987) 414–420.
[8] D.S. Green, G.A. Bickel, S.C. Wallace, J. Mol. Spectrosc. 150 (1991) 303–353.
[9] D.S. Green, G.A. Bickel, S.C. Wallace, J. Mol. Spectrosc. 150 (1991) 354–387.
[10] D.S. Green, G.A. Bickel, S.C. Wallace, J. Mol. Spectrosc. 150 (1991) 388–469.
[11] D.S. Green, S.C. Wallace, J. Chem. Phys. 96 (1992) 5857–5877.
[12] E.d. Beer, B.G. Koenders, M.P. Koopmans, C.A.d. Lange, J. Chem. Soc. Faraday Trans. 86 (1990) 2035–2041.
[13] Y. Xie, P.T.A. Reilly, S. Chilukuri, R.J. Gordon, J. Chem. Phys. 95 (1991) 854–864.
[14] E.d. Beer, W.J. Buma, C.A. deLange, J. Chem. Phys. 99 (1993) 3252–3261.
[15] Á. Kvaran, Á. Logadóttir, H. Wang, J. Chem. Phys. 109 (1998) 5856–5867.
[16] Á. Kvaran, H. Wang, Á. Logadóttir, Recent Res. Devel., in: Physical Chem., Transworld Research Network, 1998, pp. 233–244.
[17] Á. Kvaran, H. Wang, Á. Logadóttir, J. Chem. Phys. 112 (2000) 10811–10820.
[18] Á. Kvaran, H. Wang, B.G. Waage, Can. J. Phys. 79 (2001) 197–210.
[19] H. Wang, Á. Kvaran, J. Mol. Struct. 563–564 (2001) 235–239.
[20] Á. Kvaran, H. Wang, Mol. Phys. 100 (2002) 3513–3519.
[21] Á. Kvaran, H. Wang, J. Mol. Spectrosc. 228 (2004) 143–151.
[22] D. Ascenzi, S. Langford, M. Ashfold, A. Orr-Ewing, Phys. Chem. Chem. Phys. 3 (2001) 29–43.
[23] R. Liyanage, R.J. Gordon, R.W. Field, J. Chem. Phys. 109 (1998) 8374–8387.
[24] Á. Kvaran, H. Wang, K. Matthiasson, A. Bodi, E. Jónsson, J. Chem. Phys. 129 (2008) 16313.
[25] A. Kvaran, H.S. Wang, K. Matthiasson, A. Bodi, E. Jonsson, J. Chem. Phys. 129 (2008) 164313.
[26] K. Matthiasson, H.S. Wang, A. Kvaran, J. Mol. Spectrosc. 255 (2009) 1–5.
[27] A. Kvaran, K. Matthiasson, H.S. Wang, J. Chem. Phys. 131 (2009) 044324.
[28] K. Matthiasson, J.M. Long, H.S. Wang, A. Kvaran, J. Chem. Phys. 134 (2011) 164302.
[29] J. Long, H. Wang, Á. Kvaran, J. Chem. Phys. 138 (2013) 044308.
[30] R.F. Barrow, J.G. Stamper, Proc. Roy. Soc. Ser. A 263 (1961) 277–288.
[31] R.F. Barrow, J.G. Stamper, Proc. Roy. Soc. Ser. A 263 (1961) 259–276.
[32] R. Callaghan, R.J. Gordon, J. Chem. Phys. 93 (1990) 4624–4636.
[33] J.B. Nee, M. Suto, L.C. Lee, J. Chem. Phys. 85 (1986) 4919.
[34] Á. Kvaran, B.G. Waage, H. Wang, J. Chem. Phys. (2000).
[35] J. Long, H. Wang, Á. Kvaran, J. Mol. Spectrosc. 282 (2012) 20–22.
[36] J. Long, H.R. Hróðmarsson, H. Wang, Á. Kvaran, J. Chem. Phys. 136 (2012).
[37] S.G. Tilford, M.L. Ginter, A.M. Bass, J. Mol. Spectrosc. 34 (1970) 327.
[38] D.S. Ginter, M.L. Ginter, S.G. Tilford, J. Mol. Spectrosc. 92 (1982) 40.
[39] M.L. Ginter, S.G. Tilford, A.M. Bass, J. Mol. Spectrosc. 57 (1975) 271.
[40] S.A. Wright, J.D. McDonald, J. Chem. Phys. 101 (1994) 238–245.
[41] S.T. Pratt, M.L. Ginter, J. Chem. Phys. 102 (1995) 1882–1888.
[42] D.S. Ginter, M.L. Ginter, S.G. Tilford, A.M. Bass, J. Mol. Spectrosc. 92 (1982) 55.
[43] A.I. Chichinin, C. Maul, K.H. Gericke, J. Chem. Phys. 124 (2006) 224324.
[44] A.I. Chichinin, P.S. Shternin, N. Gödecke, et al., J. Chem. Phys. 125 (2006) 034310.
[45] S. Kauczok, C. Maul, A.I. Chichinin, K.H. Gericke, J. Chem. Phys. 133 (2010) 024301.
[46] C. Romanescu, S. Manzhos, D. Boldovsky, J. Clarke, H. Loock, J. Chem. Phys. 120 (2004) 767–777.
[47] H.P.L.C. Romanescu, J. Chem. Phys. 127 (2007) 124304.
[48] C. Romanescu, H.P. Loock, Phys. Chem. Chem. Phys. 8 (2006) 2940–2949.
[49] Á. Kvaran, K. Matthíasson, H. Wang, Phys. Chem. Ind. J. 1 (2006) 11–25.
[50] Á. Kvaran, Ó.F. Sigurbjörnsson, H. Wang, J. Mol. Struct. 790 (2006) 27–30.
[51] NIST (National Institute of Standards and Technology), http://webbook.nist.gov/chemistry/form-ser.html.en-us.en>.
[52] H.R. Hróðmarsson, Á. Kvaran, H. Wang, unpublished, (2013).